Check for updates

Received: 28 February 2026 | Revised: 27 June 2026 | Accepted: 8 October 2026

DOI: 10.1002/dvdy.70200

RESEARCH ARTICLE

Developmental Dynamics | American Association for Anatomy | WILEY

Different from bone: Tooth formation and enameloid mineralization are not affected by reduced dietary phosphorus intake

S. Cotti[1,2] | A. Huysseune[1] | I. A. K. Fiedler[3] | B. Busse[3] | C. Di Biagio[4] | M. Rücklin[5,6] | F. Marone[7] | A. Forlino[2] | P. E. Witten[1]

[1]Biology Department, Evolutionary Developmental Biology, Ghent University, Ghent, Belgium

[2]Department of Molecular Medicine, Biochemistry Unit, University of Pavia, Pavia, Italy

[3]Department of Osteology and Biomechanics, University Medical Center Hamburg-Eppendorf, Hamburg, Germany

[4]Department of Biology, University of Rome Tor Vergata, Rome, Italy

[5]Naturalis Biodiversity Center, Leiden, The Netherlands

[6]Institute of Biology, Leiden University, Leiden, The Netherlands

[7]X-ray Tomography Group, Swiss Light Source, Paul Scherrer Institut, Villigen, Switzerland

Correspondence
P. E. Witten, Biology Department, Evolutionary Developmental Biology, Ghent University, 9000 Ghent, Belgium.
Email: peckhardwitten@aol.com

Funding information
Ghent University, Bijzonder Onderzoeksfonds, Grant/Award Number: BOF.ITN.2021.0012.01; HORIZON EUROPE Marie Skłodowska-Curie Actions, Grant/Award Number: 766347 (Biomedaqu)

Abstract

Background: Vertebrates rely on phosphorus intake for skeletal mineralization. In humans, hypomineralized teeth associated with rickets, hypophosphatemia, hypophosphatasia, or idiopathic molar-incisor-hypomineralization pose significant problems. Here tooth development in wild-type zebrafish and in osteocalcin GFP reporter-line zebrafish is examined under conditions of low, regular, and high dietary phosphorus (P) intake. Mineralization of tooth and jaw bone matrices was analyzed by Alizarin red S staining, synchrotron X-ray tomography, Von Kossa staining of histological sections, Raman micro-spectroscopy, nanoindentation, phosphate transporter gene expression detection, and additional histological techniques.

Results: Tooth development, enameloid and dentin formation, and bone matrix deposition proceed uninterrupted in zebrafish fed a low phosphorus diet. However, P-deficiency impairs bone matrix mineralization, dentin mineralization is delayed, and enameloid mineralization remains unaffected. Raman spectroscopy on erupted teeth reveals no changes in dentin mineral composition. The vectorial Na-P co-transporter *slc34a2b* is expressed in ameloblasts, which agrees with the cells' known contribution to enameloid mineralization.

Conclusions: It is hypothesized that active phosphate transport by ameloblasts possibly also contributes to the mineralization of dentin. The observed uncoupling of bone and tooth mineralization aligns with findings in other teleost species under natural conditions, and with laboratory studies on zebrafish and mammals that impair bone mineralization.

KEYWORDS

dentin, enameloid, mineralization, phosphorus, zebrafish teeth

This is an open access article under the terms of the Creative Commons Attribution-NonCommercial-NoDerivs License, which permits use and distribution in any medium, provided the original work is properly cited, the use is non-commercial and no modifications or adaptations are made.

© 2026 The Author(s). *Developmental Dynamics* published by Wiley Periodicals LLC on behalf of American Association for Anatomy.

INTRODUCTION

Studies on various teleost species have revealed a dramatic impact of a low dietary P intake on mineralization, both of the dermal skeleton (elasmoid scales and dermal fin rays) as well as the endoskeleton (notably the vertebral column). During periods of low dietary P intake, vertebrae continue to grow, but the matrix remains non-mineralized. Likewise, scales continue to grow with regular scale ring formation, and also the growth of dermal fin rays continues, but their matrices remain non-mineralized.[1–5] Like scales and fin rays, teeth are elements of the dermal skeleton, requiring both an epithelium and mesenchyme for their formation. As a mineralized skeleton, the dermal skeleton is older than the endoskeleton.[6] Because primary aquatic gnathostomes are largely independent from dietary calcium supply, it is currently hypothesized that P storage, and not the storage of calcium, was an initial function of the dermal skeleton.[7,8] If and to what extent a low dietary P supply affects tooth formation in teleost fish is not known. Experiments on rodents have shown that incisor growth and mineralization are largely independent from reduced dietary P intake, provided the animals receive enough calcium.[9–11] In humans, however, P metabolism-related disorders can cause tooth hypomineralization, including numerous types of hypophosphatemia, hypophosphatasia and idiopathic molar-incisor hypomineralization.

This study addresses the effects of low and high dietary P intake on tooth development, tooth replacement, tooth structure and tooth mineralization in a teleost model with a well-studied dentition, the zebrafish (*Danio rerio*). Different from mammals that only have one or two tooth generations, zebrafish—like most other non-mammalian vertebrates—replace teeth lifelong. In zebrafish, tooth replacement is frequent and rapid. This facilitates experimental studies on tooth formation in adult individuals. On the downside, zebrafish teeth are 15–20 times smaller than lower mouse incisors, and cells are only half the size of mammalian cells. This increases the workload of analytics, and often standard protocols have to be adapted.[12] Here, the analysis of zebrafish tooth development is based on the impact of three custom designed diets with low, regular and high phosphorus content (LP, RP and HP, respectively), fed to wild type and osteocalcin:GFP (*osc*:GFP) transgenic zebrafish. The teeth are analyzed using a combination of whole mount staining, histology, synchrotron X-ray tomography, Raman microspectroscopy, and nanoindentation, along with localizing the expression of osteocalcin and *slc34a2b*, encoding a vectorial epithelial P transporter. This combined approach reveals fundamental differences in the behavior of bone, dentin and enameloid with respect to low levels of dietary phosphorus supply.

RESULTS

Low dietary P-intake does not inhibit tooth development

Zebrafish, like other cyprinids, have ventral pharyngeal teeth, associated with the fifth ceratobranchials (the pharyngeal jaw bones), and arranged in three rows (Figure 1A–C). This study focuses on the ventral tooth row (Figure 1C,D), which is the most thoroughly investigated.[14–16] Tooth anlagen and developing teeth were present in all groups, including the LP group (Figure 1E–G). Considering that a tooth replacement cycle in juveniles lasts about 8 days and larger teeth replace the lost ones,[14,17] it is safe to conclude that the teeth examined after 1 or 2 months of dietary treatment developed during the experimental period. Comparison of the size of the five ventral teeth (1V–5V) at the beginning (T0) and at the end of the experiment confirmed that larger ventral teeth were present after 2 months of dietary treatment. Neither reduced nor elevated dietary P intake had an effect on tooth formation per se or tooth size.

Tooth attachment

Within the LP group, about half of the five ventral teeth analyzed were attached via a non-mineralized pedicel (Figure 1E,H). In contrast, in RP and HP zebrafish, the majority of the ventral teeth had a fully mineralized pedicel (also commonly referred to as bone of attachment[18]) after one (RP: 71%; HP: 61%) and after 2 months (RP: 85%; HP: 87%) of dietary treatment (Figure 1F–H). A Chi-square test followed by Bonferroni correction showed that the fraction of teeth attached via a non-mineralized pedicel was significantly higher in LP animals compared to RP and HP animals at both time points (Figure 1H).

Mineralization: dentin, pedicel and bone

The extent of mineralization was visualized by whole mount Alizarin red S staining of a total of 112 specimens (1120 teeth), allowing statistical treatment of the data (Figure 1E–H). Qualitative analyses were based on synchrotron X-ray tomography (Figure 2A–F) and on Von Kossa/Van Gieson staining (Figure 2G–O). One and 2 months of LP diet strongly reduced mineralization of

10970177, 0, Downloaded from https://anatomypubs.onlinelibrary.wiley.com/doi/10.1002/dvdy.70200 by Naturalis Biodiversity Center, Wiley Online Library on [10/11/2026]. See the Terms and Conditions (https://onlinelibrary.wiley.com/terms-and-conditions) on Wiley Online Library for rules of use; OA articles are governed by the applicable Creative Commons License

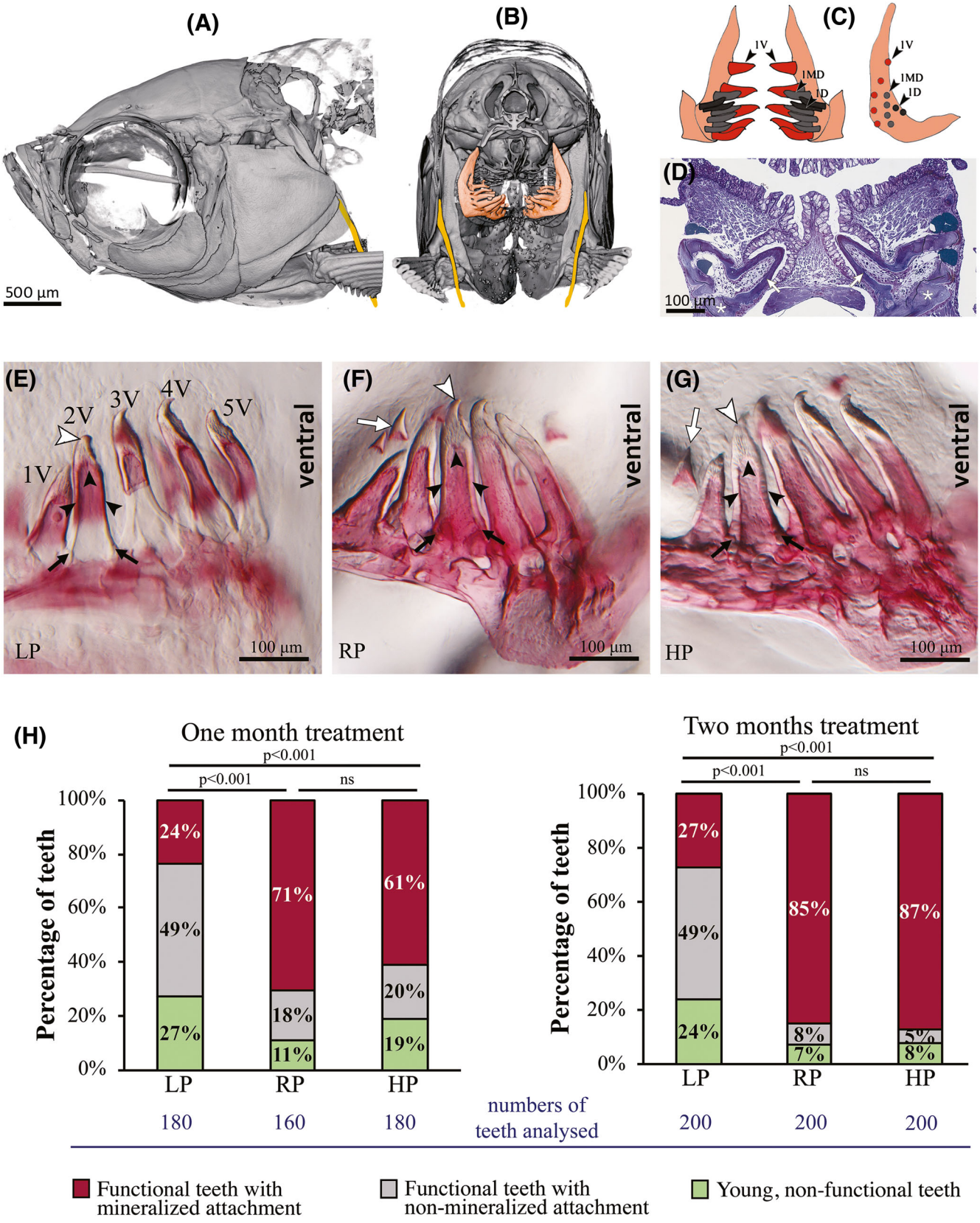


FIGURE 1 Legend on next page.

10970177, 0, Downloaded from https://anatomypubs.onlinelibrary.wiley.com/doi/10.1002/dvdy.70200 by Naturalis Biodiversity Center, Wiley Online Library on [10/11/2026]. See the Terms and Conditions (https://onlinelibrary.wiley.com/terms-and-conditions) on Wiley Online Library for rules of use; OA articles are governed by the applicable Creative Commons License

the jaw bones and the proximal parts of all teeth (Figures 1E and 2A,D). No substantial differences in mineralization could be observed between teeth from RP and HP animals based on Alizarin red S staining (Figure 1F,G). Individual teeth analyzed by synchrotron X-ray tomography showed no mineralization differences between the individuals from the RP and the HP group (Figure 2B,C,E,F). Histological sections stained with Von Kossa and Van Gieson confirmed the mineralization pattern observed on synchrotron X-ray tomography scans (Figure 2G–I).

In contrast to normal zebrafish dentinogenesis, whereby non-mineralized predentin becomes rapidly mineralized after its initial deposition,[15,16] the dentin of newly erupted teeth from LP animals started to mineralize but large amounts of non-mineralized dentin persisted. Synchrotron imaging showed that only the peripheral dentin was mineralized (Figure 2D). Despite reduced dentin mineralization in LP animals, mineralization continued during the functional lifetime of LP teeth (Figure 2J,M). In contrast, dentin of newly erupted teeth from RP and HP animals was more homogeneously mineralized (Figure 2K,L,N,O).

Independent from the degree of mineralization, ventral teeth (1V, 2V and 3V) in all dietary groups presented a similar dentin thickness (Table S1). Toluidine blue stained sections prepared from tooth 1V, previously processed for synchrotron X-ray tomography imaging (Figure 3A,E,I) showed polarized odontoblasts with odontoblast processes extending into the dentin in animals from all three diet groups (Figure 3B,C,F,G,J,K). The dentin showed a smooth surface down to the cervical loop in contact with the inner dental epithelium. Beyond the cervical loop, the pedicel enveloping the dentin base had a scalloped outer surface, more pronounced in the LP diet group tooth, but present also in the RP and HP diet group teeth (Figure 3B,F,J). Cells in this region did not extend tubules into the matrix, unlike odontoblasts. Under polarized light, the matrix of the pedicel showed parallel oriented collagen fibrils, different from the birefringence of the dentin (Figure 3M–O). The boundary between the pedicel and the jaw bone could be recognized by (i) the change in morphology of the pseudo-epithelium at the pulpal side, (ii) the corresponding transition from a scalloped to a smooth matrix surface at the outside, and (iii) the appearance of osteocytes in the bone (Figure 3B,M,N).

Dental tissues and enameloid mineral composition and hardness

Raman micro-spectroscopy showed that all tissues shared a similar spectroscopic fingerprint region. Specifically, the presence and spectral location of phosphate, carbonate, amide I, amide III, and CH_2 peaks were similar between the dietary groups (Figure 4A).

As expected, under all dietary conditions the enameloid showed a higher degree of mineralization than dentin, pedicel, and pharyngeal bone. This is reflected by the protein-related spectral ranges of CH_2 and amide I which were reduced relative to phosphate in enameloid compared to the other tissues (Figure 4B). Spectral quantification yielded that the phosphate/amide III ratio of enameloid was more than two-fold higher than that of dentin ($p = .05$), pedicel ($p = .0003$), and pharyngeal bone ($p = .0008$). Similarly, the phosphate/CH_2 ratio was higher in enameloid compared to the other three types of skeletal tissues (Figure 4C). The carbonate/amide I ratio showed the lowest values in dentin, and a trend towards a higher ratio in pedicel and pharyngeal bone in all dietary groups. The highest ratio was recorded in enameloid, with a carbonate/amide ratio significantly higher than in dentin ($p = .0393$, Figure 4D). The carbonate/phosphate ratio, a measure of mineral maturity, was significantly higher in pharyngeal bone versus dentin

FIGURE 1 (A) Zeiss Xradia Micro CT-scan (voxel size 4 μm) of the head of an adult zebrafish, lateral view. The cleithrum (highlighted in yellow) indicates the position, on an antero-posterior axis, of the pharyngeal jaws. (B) Same scan as in A, caudal view on the occipital region of the skull, the shoulder girdle and the pharyngeal tooth-bearing jaws (pink). Cleithra are labeled yellow, as in (A). (C) Left image, dorsal view on the pharyngeal jaws, showing the 11 zebrafish tooth positions on each of the jaws. Ventral tooth row in red (V), mediodorsal tooth row in gray (MD), and dorsal tooth row in black (D). Right image, medial view of right jaw, indicating the position of the five ventral teeth (1V–5V), the four mediodorsal teeth (1MD–4MD) and the two dorsal teeth (1D–2D). Arrowheads indicate the first tooth of the respective tooth row, modified after.[13] (D) Cross section, tooth-bearing pharyngeal region. Three-month old zebrafish. Two erupted teeth of the ventral row (1V, white arrows), pharyngeal jaw bones (white asterisks), toluidine blue staining. (E–G) Alizarin red S stained pharyngeal jaws with five ventral teeth (1V–5V) in LP, control (RP) and HP after 2 months of dietary treatment; developing replacement teeth indicated by white arrows. Hypermineralized enameloid (white arrowheads) does not take up Alizarin red S. (E) LP fish show reduced pedicel mineralization (black arrows), mineralized dentin (black arrowheads), fully mineralized enameloid (white arrowhead). (F, G) RP and HP teeth are attached via a fully mineralized pedicel (black arrows). (H) Fraction of the ventral tooth row presenting either young (non-functional) teeth, or functional teeth with non-mineralized or with mineralized tooth attachment, after 1 and 2 months of dietary treatment. The fraction of teeth attached via a non-mineralized pedicel is larger in the LP group compared to RP and HP. Number of teeth analyzed as indicated. Chi-square test followed by Bonferroni correction, *p*-values relative to the mineralization of the pedicel are indicated, ns: non-significant.

10970177, 0, Downloaded from https://anatomypubs.onlinelibrary.wiley.com/doi/10.1002/dvdy.70200 by Naturalis Biodiversity Center, Wiley Online Library on [10/11/2026]. See the Terms and Conditions (https://onlinelibrary.wiley.com/terms-and-conditions) on Wiley Online Library for rules of use; OA articles are governed by the applicable Creative Commons License

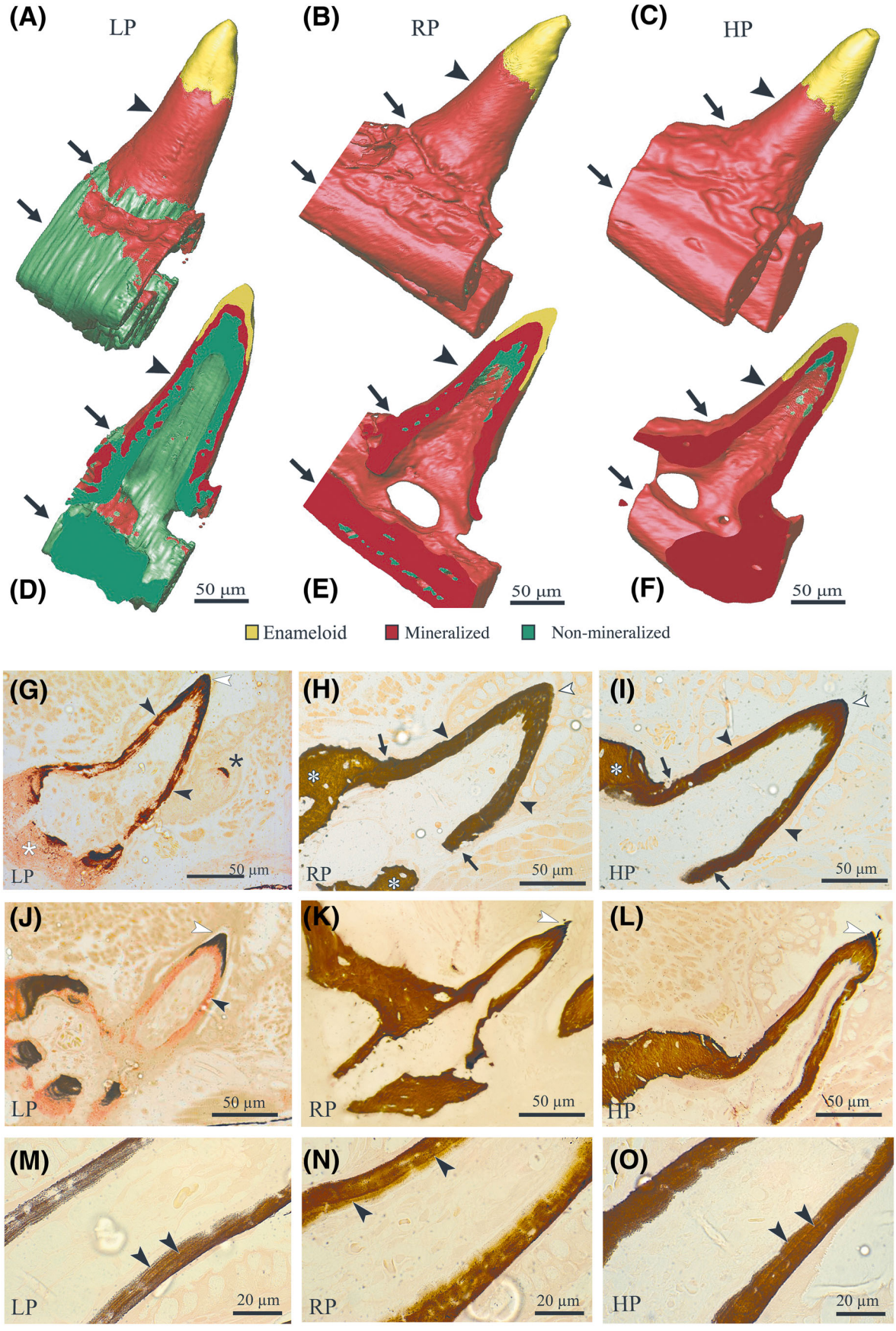


FIGURE 2 Legend on next page.

10970177, 0, Downloaded from https://anatomypubs.onlinelibrary.wiley.com/doi/10.1002/dvdy.70200 by Naturalis Biodiversity Center, Wiley Online Library on [10/11/2026]. See the Terms and Conditions (https://onlinelibrary.wiley.com/terms-and-conditions) on Wiley Online Library for rules of use; OA articles are governed by the applicable Creative Commons License

($p = .0053$, Figure 4E). Crystallinity, a measure of crystal size, showed the highest values in enameloid compared to pharyngeal bone ($p = .003$, Figure 4F).

Independent of the dietary group, nanoindentation tests revealed that pharyngeal bone had a higher tissue level stiffness (assessed as elastic modulus) compared to the pedicel ($p = .0014$), and a trend towards higher stiffness compared to dentin ($p = 0.0563$) (Figure 4G,H). Yet, dental tissues showed a higher hardness in the HP group compared to the RP group ($p = .0195$, Figure 4I), and higher tissue level stiffness in the HP group compared to the RP and the LP group ($p = .0265$ and $p = .0118$, respectively, Figure 4J). The mineral-to-matrix ratio, carbonate-to-amide I ratio, or crystallinity of zebrafish dental tissues, assessed by Raman spectroscopy, did not reveal any significant effect of diet (Figure 4B–F). However, a trend towards an effect of diet was observed in the mineral-related parameters of the pedicel. Specifically, the mineral within the pedicel showed higher mean carbonate/phosphate ratios with higher P-content in the diet which were accompanied by lower means in crystallinity with increasing P-content (Figure 4E,F).

Osteocalcin expression in odontoblasts, osteoblasts and osteocytes

Given the impact of P deficiency on dentin mineralization, we examined whether the expression of osteocalcin in odontoblasts depends on dietary P intake. In an earlier study, an increase of expression in bone of LP animals was measured for *col1a1a* and *osteocalcin*, related to the upregulation of bone matrix formation.[4] Osteocalcin (also known as bone gamma-carboxyglutamate [Gla] protein) is a non-collagenous protein produced by osteoblasts, osteocytes and odontoblasts and present in mammalian tooth and bone matrix.[20] To assess the expression of osteocalcin in zebrafish dental tissues, an *osc*:GFP reporter line was used. Irrespective of the level of P intake, after 2 months of treatment osteocalcin was expressed in odontoblasts, in osteoblasts, osteocytes and in bone lining cells in all dietary groups (Figure 5A–D). An osteocalcin:GFP signal labeled also odontoblast and osteocyte processes within the dentin and bone matrix, respectively (Figure 5B,C). No osteocalcin expression was detectable in ameloblasts at any stage of tooth development in any of the dietary groups. To compare the effect of P deficiency on osteocalcin expression in more detail, the extent of the GFP signal was measured within the pulp cavity of two teeth in a comparable developmental stage in all dietary groups, with the area normalized to the pulp cavity area: a replacement tooth in position 3V and a young functional tooth in position 1V. No significant difference was detected among dietary groups in the GFP signal area within the pulp cavity of the young functional tooth 1V and the replacement tooth 3V (Table S2).

Enameloid mineralization and epithelial P transporter expression

Alizarin red S staining, synchrotron X-ray tomography, Von Kossa-stained histological sections, and Raman spectroscopy showed that enameloid mineralization was unaffected by low dietary P intake (Figures 1E, 2A,D,G, and 4C–F).

This finding raised the question if mineralization mechanisms of enameloid are distinct from those of bone and dentin, as this is the case for enamel. To support the view that enameloid mineralization in zebrafish is facilitated by active ameloblast (epithelial) transport of P from plasma or from water, the expression of a gene coding for

FIGURE 2 (A–C) Synchrotron X-ray tomographic microscopy 3D reconstructions and (D–F) virtual sections of the erupted, fully functional tooth 1V in LP, RP and HP zebrafish. Hypermineralized enameloid yellow, mineralized tissue red, non-mineralized tissue green. Differences in dentin and jaw bone mineralization are prominent in LP fish but all teeth have a similar size and a similar-sized enameloid cap. In LP animals, dentin mineralization is restricted to the outer dentin areas (black arrowhead), pedicels and jaw bones remain largely non-mineralized (black arrows). Teeth from RP and HP animals with fully mineralized dentin (black arrowheads), pedicel and jaw bone (black arrows) with a small area of non-mineralized predentin at the tip of the pulp cavity. (G–I) Von Kossa/Van Gieson stained non-demineralized sections of ventral tooth 1V. Dark staining, mineralized tissue; pink areas non-mineralized collagen. Note partly mineralized dentin (black arrowheads) and non-mineralized jaw bone (white asterisk) in the LP fish. The black asterisk indicates a developing tooth with densely mineralized enameloid cap (G), compared to fully mineralized dentin (black arrowheads), pedicel (black arrows) and jaw bone (white asterisks) in RP (H) and HP fish (I). Enameloid is densely mineralized (white arrowhead) in all three conditions. (J–L) Non-demineralized Von Kossa/Van Gieson stained sections from a newly erupted tooth in an LP (J), RP (K) and HP (L) animal. Note fully mineralized enameloid cap (white arrowhead) in teeth from all diet groups, but teeth from LP fish (J) lack minerals in the dentin (black arrowhead), in contrast to fully mineralized dentin in RP and HP fish (K, L). Mineralization of dentin in LP teeth is delayed but will continue, albeit at a lower level, compare (J) with (G). (M–O) Higher magnifications reveal darker staining lines within the dentin (black arrowheads) orientated parallel to the long axis of the teeth in animals from all dietary groups, possibly related to intermittent mineralization.

10970177, 0, Downloaded from https://anatomypubs.onlinelibrary.wiley.com/doi/10.1002/dvdy.70200 by Naturalis Biodiversity Center, Wiley Online Library on [10/11/2026]. See the Terms and Conditions (https://onlinelibrary.wiley.com/terms-and-conditions) on Wiley Online Library for rules of use; OA articles are governed by the applicable Creative Commons License

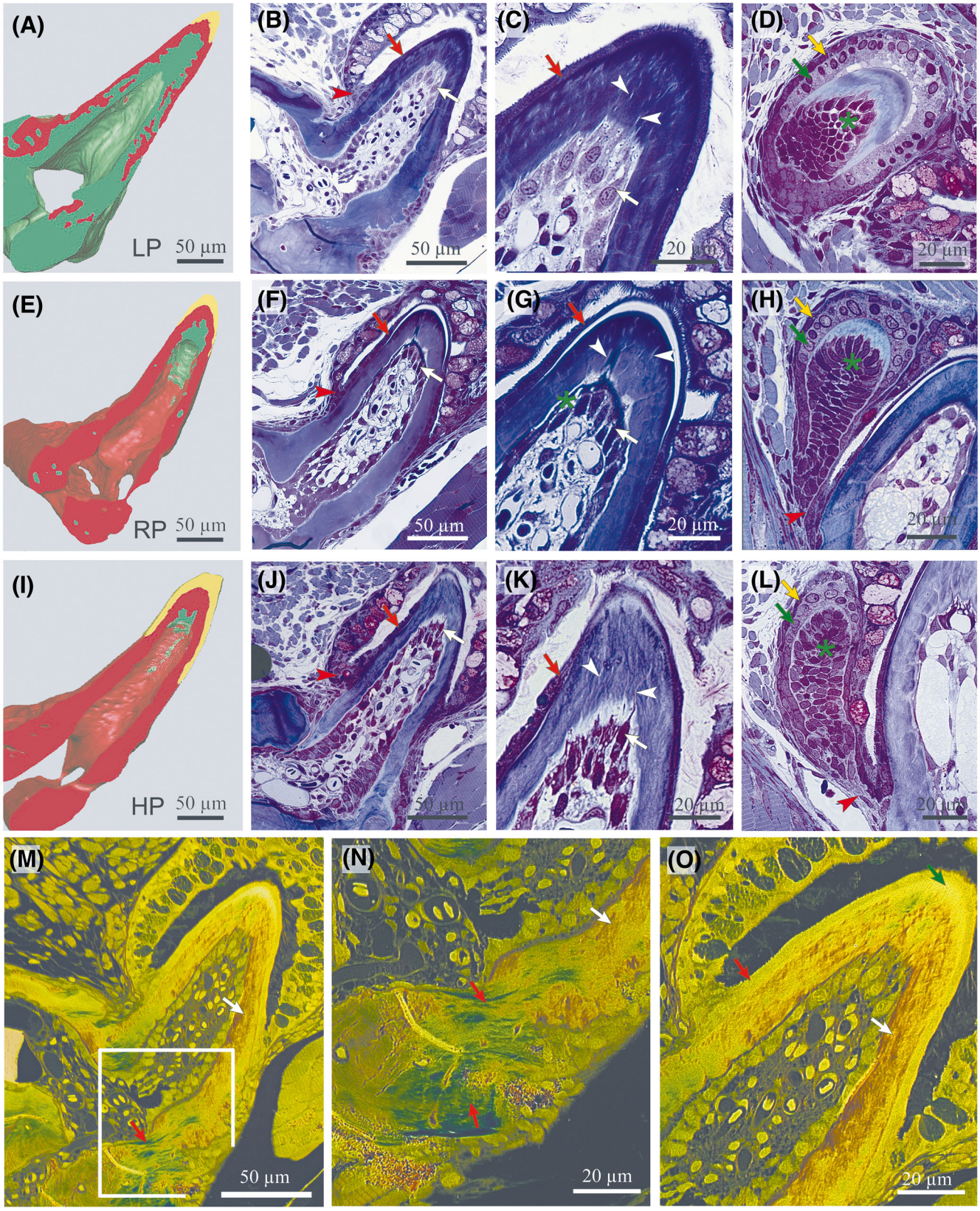


FIGURE 3 Legend on next page.

10970177, 0, Downloaded from https://anatomypubs.onlinelibrary.wiley.com/doi/10.1002/dvdy.70200 by Naturalis Biodiversity Center, Wiley Online Library on [10/11/2026]. See the Terms and Conditions (https://onlinelibrary.wiley.com/terms-and-conditions) on Wiley Online Library for rules of use; OA articles are governed by the applicable Creative Commons License

the vectorial Na-P co-transporter *slc34a2b* was assessed by in situ hybridization. *slc34a2b* was chosen based on its conservation across vertebrates and on the specific expression of this Na-P co-transporter in murine ameloblasts.[21,22] Analysis of whole mount in situ hybridization and subsequent sections from zebrafish teeth from all three dietary groups revealed a distinct localization of *slc34a2b* at the tooth tips (Figure 5F–H). A semi-quantitative analysis of possible different levels of expression in LP, RP, and HP animals was not performed. The *slc34a2b* signal was specific and well distinguishable from the background. No *slc34a2b* was observed in odontoblasts, osteoblasts, or osteocytes (Figure 5F). There was a clear distinction between the osteocalcin signal, exclusively observed in the odontoblasts, and the *slc34a2b* signal, expressed in ameloblasts (Figure 5D–F). The known expression of *slc34a2b* in the cells of the zebrafish gill epithelium was also confirmed (Figure 5I).[23]

DISCUSSION

Teleost fish and other primary aquatic jawed vertebrates (gnathostomes) are largely independent from dietary calcium intake.[24,25] In addition to intestinal calcium absorption and renal excretion, calcium can be absorbed from, and excreted into, the water by active gill epithelium transport. In contrast, P absorption from the water is possible but insufficient to fulfill the animals' P-requirement. Hence, P remains as a critical dietary parameter for the mineralization of the calcium phosphate-based skeleton.[2,8,26] In mammals, insufficient P intake causes hypomineralized bones, a condition known as osteomalacia.[27] In this study on zebrafish, it is demonstrated that a period of reduced dietary P intake also causes osteomalacia. The P-reduction prevents jaw bone and pedicel mineralization; mineralization of dentin is less affected and enameloid mineralization is unaffected. Independent from mineralization, bone and dentin matrix formation and tooth replacement continue normally. Below, the divergent effects of low dietary P intake on bone and tooth formation are discussed, as well as the apparently dietary P-independent mineralization of enameloid.

Independent bone and tooth mineralization

Previous studies on vertebral bodies in Atlantic salmon (*Salmo salar*) and zebrafish subjected to periods of reduced dietary P intake have shown that the bone of vertebral bodies continues to grow but new bone remains non-mineralized, resulting in an osteomalacia-like condition.[1,3,5] In zebrafish, bone matrix production is even stimulated.[4] In both species, zebrafish and salmon, the large amount of non-mineralized bone matrix mineralizes as soon as the animals return to a P-sufficient diet.[2,4] Evidently, non-mineralized teeth would be non-functional. LP zebrafish have erupted teeth with mineralized enameloid and mineralized dentin surfaces, but only partially mineralized jaw bones, indicating that teeth and bone mineralization are uncoupled. Other studies have shown a similar uncoupling. Zebrafish *no bone* (NOB) mutants are defective for ectonucleoside triphosphate/diphosphohydrolase 5 (*entpd5*), an enzyme that hydrolyzes the potent mineralization inhibitor pyrophosphate. With pyrophosphate persisting in the matrix, bones do not mineralize. Still, NOB zebrafish maintain the ability to develop mineralized teeth.[28] The synthesis of pyrophosphate itself depends on the *enpp1* gene, encoding ectonucleotide pyrophosphatase phosphodiesterase 1, a membrane-bound ectoenzyme. *ENPP1* mutations in humans cause autosomal recessive hypophosphatemic rickets type 2, associated with skeletal hypermineralization and arterial calcification. The *Enpp1*-null mouse recapitulates the human hypermineralization phenotype, but again, without impact on enamel or dentin mineralization.[29]

FIGURE 3 (A–C) Erupted tooth 1V of an LP animal, shown as virtual synchrotron X-ray tomography section (color code as in Figure 2A–F). (B, C) Demineralized histological sections from the same tooth. (D) Replacement tooth in an LP animal. (E–G) Erupted tooth 1V of an RP animal, shown as in (A–C). (H) Replacement tooth in an LP animal. (I–K) Erupted tooth 1V of a HP animal, shown as in (A–C). (L) Replacement tooth in a HP animal. None of the sections in (B, C, F, G, J, K) passes through the tooth tip, preventing observations on the enameloid cap. In animals from all three diet groups, odontoblasts (white arrows) extend cell processes into the dentin (white arrowheads), and flattened cells of the inner dental epithelium cover the tooth shaft (red arrows). The position of the cervical loop (red arrowheads) matches the basis of the tooth, at the level of the boundary with the pedicel/bone of attachment. (D, H, L) In all three diet groups replacement teeth derive from the outer dental epithelium (red arrowheads) of the erupted teeth (not visible in D). Inner (green arrow) and outer dental epithelium (yellow arrow) are indicated. Pulp cavities are filled with mesenchymal cells that have started to differentiate into odontoblasts (green asterisks). The replacement tooth depicted in (L) is in an earlier stage of differentiation compared to the replacement teeth shown in (D and H). (M) Tooth 1V shown in (B), visualized with polarized light revealing the different orientation of collagen fibers in the pedicel (red arrow) and dentin (white arrow). (N) Higher magnification of the boxed area in (M); collagen fibers in the pedicel (red arrows) and dentin (white arrow). (O) Higher magnification of the tooth shown in (M). The red arrow indicates the inner dental epithelium. The green arrow indicates the non-birefringent tooth surface (possibly collar enameloid[19]), in contrast to the birefringent dentin (white arrow).

10970177, 0, Downloaded from https://anatomypubs.onlinelibrary.wiley.com/doi/10.1002/dvdy.70200 by Naturalis Biodiversity Center, Wiley Online Library on [10/11/2026]. See the Terms and Conditions (https://onlinelibrary.wiley.com/terms-and-conditions) on Wiley Online Library for rules of use; OA articles are governed by the applicable Creative Commons License

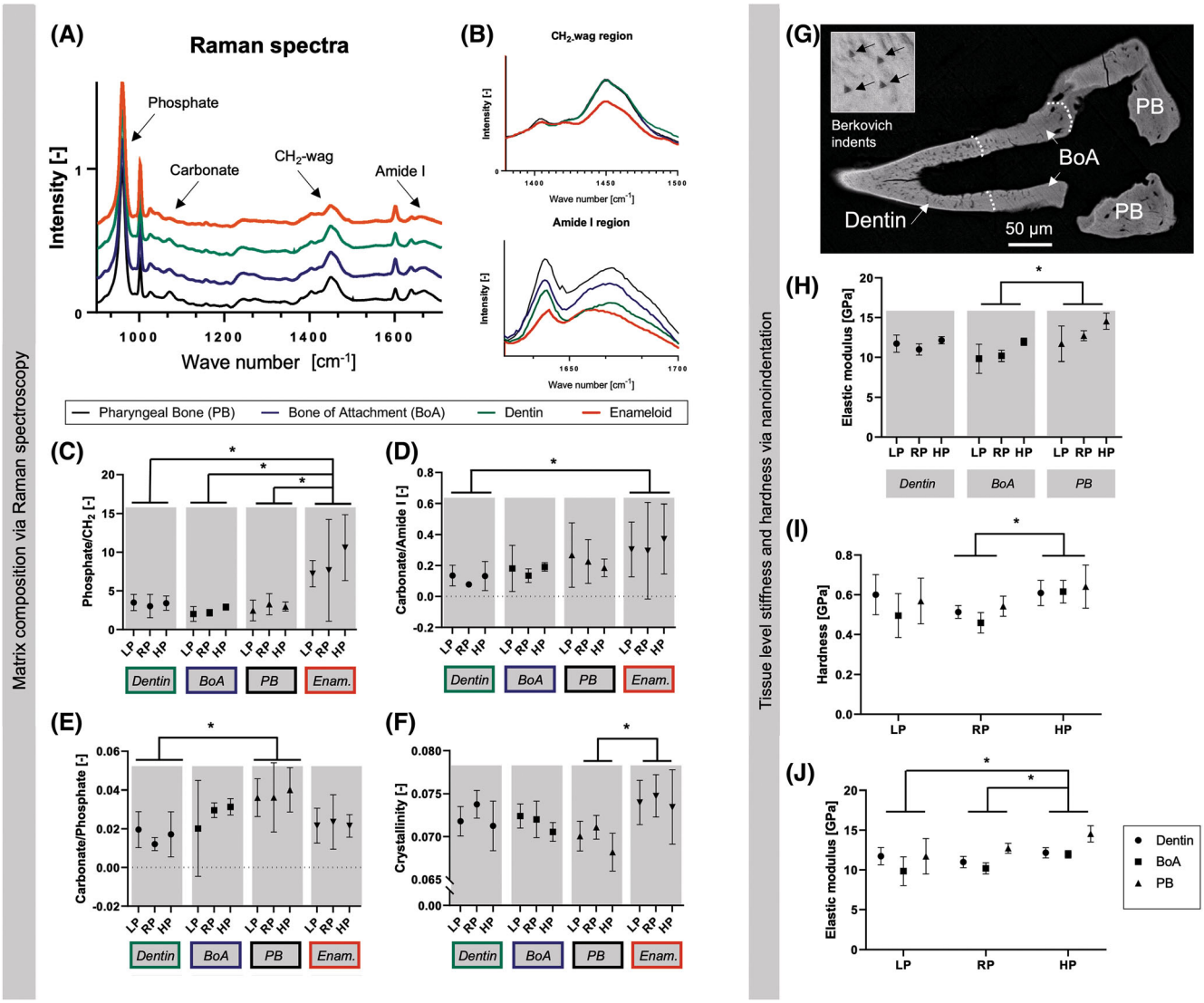


FIGURE 4 Raman spectroscopic analysis for tissue quality and nanoindentation tests for mechanical properties. (A) Raman spectra averaged for each tissue measured; pharyngeal bone (PB), pedicel (bone of attachment, BoA), dentin, and enameloid show similar fingerprint. (B) Magnified spectral range of the CH_2-wag and amide I envelope indicate lower protein content in enameloid compared to the other tissues. (C) Enameloid is significantly more mineralized compared to dental tissues (assessed in terms of a mineral-to-matrix ratio, e.g., phosphate/CH_2). (D) The carbonate to amide I ratio is significantly higher in enameloid compared to dentin. (E) Pharyngeal bone shows a significantly higher carbonate/phosphate ratio (i.e., type B carbonate substitution in the mineral lattice) compared to dentin. (F) A lower crystallinity of dentin compared to enameloid. No significant effects induced by diet were found. (G) Backscattered electron image showing the regions of interest for placing the indents in dentin, pedicel (bone of attachment, BoA) and pharyngeal bone (PB). (H) Tissue level stiffness, assessed as elastic modulus, is significantly higher in PB than in BoA. (I) Independent of the tissue, high P diet resulted in higher tissue level hardness compared to regular P diet. (J) Tissue level stiffness, assessed as elastic modulus is significantly higher in the high P-diet group compared to the RP and LP group.

Cell and tissue reactions to alteration in dietary P intake

In line with observations made on the vertebral bone of zebrafish subjected to diets with different phosphorus content, we found higher tissue level stiffness in dental tissues of zebrafish in response to higher dietary P content. A lower elastic modulus is often correlated with a lower mineral-to-matrix ratio, a lower carbonate/phosphate ratio (i.e., the relative amount of type-B-carbonate substitution within the mineral lattice), and lower crystallinity.[30] In the present study, the observed effects of dietary P-content on the mechanical properties of the dental tissues were not related to significant alterations in the matrix composition of the different tissues, although a higher degree of mineralization or type-

10970177, 0, Downloaded from https://anatomypubs.onlinelibrary.wiley.com/doi/10.1002/dvdy.70200 by Naturalis Biodiversity Center, Wiley Online Library on [10/11/2026]. See the Terms and Conditions (https://onlinelibrary.wiley.com/terms-and-conditions) on Wiley Online Library for rules of use; OA articles are governed by the applicable Creative Commons License

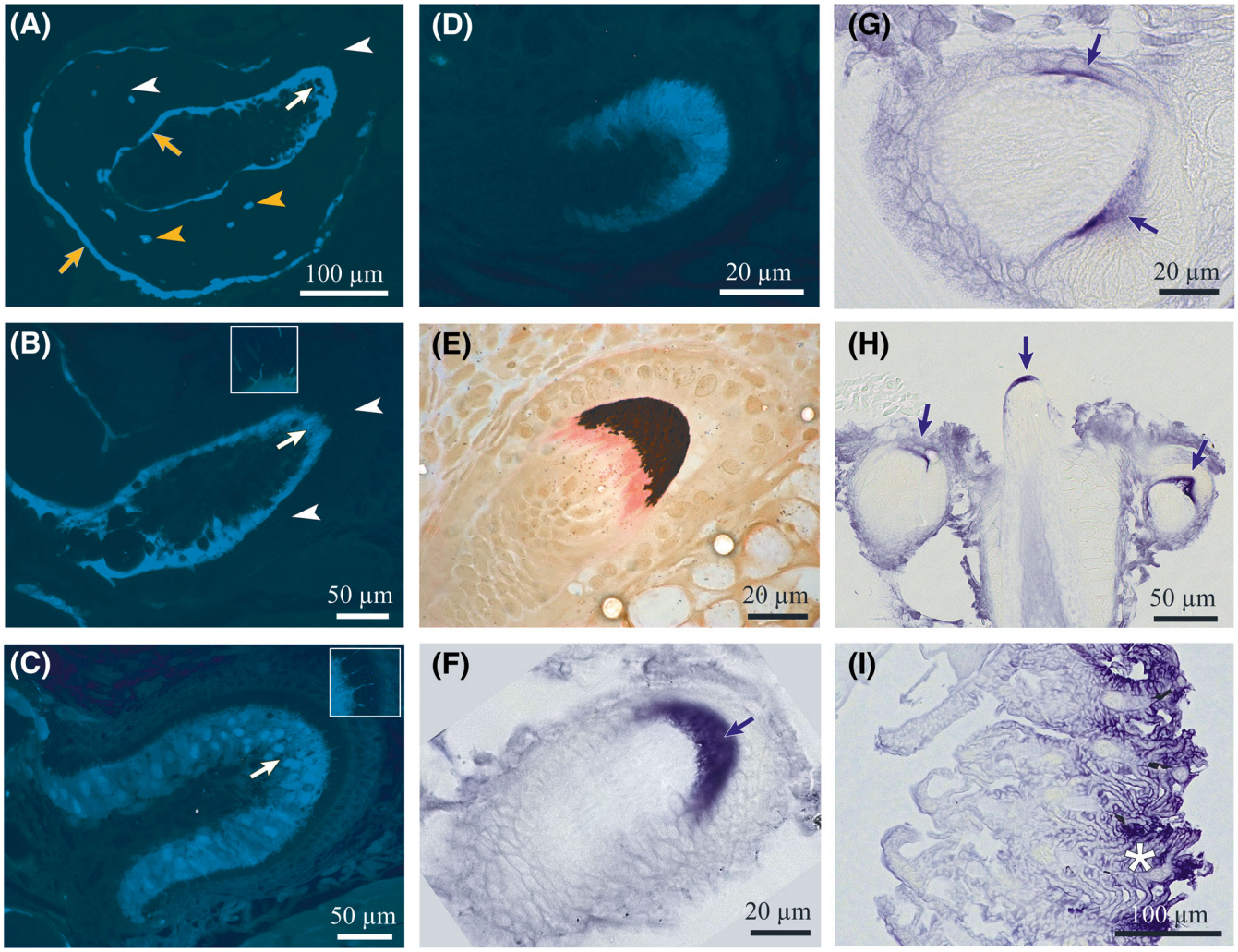


FIGURE 5 Osteocalcin and Na-P co-transporter *slc34a2b* expression. (A–D) Expression of osteocalcin in cells forming dental tissues in zebrafish. Osteocalcin expression is homogeneous in all dietary groups, represented here by sections from LP diet animals. (A) Basis of erupted tooth 1V with adjacent jaw bone. Osteocalcin expression is specific and located in osteocytes (yellow arrowheads), osteoblasts (yellow arrows), and odontoblasts (white arrow). White arrowheads indicate osteocyte and odontoblast processes. (B) Dentin and pulp cavity of tooth 1V. Osteocalcin expression by odontoblasts (white arrow). White arrowheads indicate odontoblast processes, also shown in the insert at higher magnification. (C) Replacement tooth 3V in late cytodifferentiation stage, with osteocalcin expression in the odontoblasts (white arrow). In all stages of tooth development, the cells of the enamel organ are osteocalcin-negative. The insert shows odontoblast processes at higher magnification. (D, E) Early stages of replacement tooth development, unaffected by the LP diet, showing distinct expression of osteocalcin in odontoblasts but not in ameloblasts (D), and regular mineralization of enameloid (E). (F–I) Localization of the vectorial Na-P co-transporter *slc34a2b* by in situ hybridization in replacement teeth of different stages of development. *slc34a2b* transcripts are localized at tooth tips covered by ameloblasts (blue arrows). Ameloblasts stain positive for *slc34a2b* in early (F, G) and also in later stages of tooth development (H). Odontoblasts do not express *slc34a2b*. (I) *slc34a2b* expression is also prominent in cells of the gill epithelium. The white asterisk labels the gill lamellae.

B-carbonate substitution could be expected in the dentin, pedicel and pharyngeal bone of the HP group compared to the LP and RP groups. Interestingly, the pedicel showed higher means in its carbonate/phosphate ratios, suggesting higher type-B-carbonate substitution within the mineral lattice, but lower means in crystallinity. Such inverse behavior, that is, a higher carbonate substitution combined with a lower crystallinity, has previously been described in vertebral bone of a zebrafish model of osteogenesis imperfecta, which is characterized by a less mature matrix and rampant mineralization.[31] Such behavior might suggest a specific role of the pedicel in the scope of P-dependent mineralization mechanisms in zebrafish teeth.

10970177, 0, Downloaded from https://anatomypubs.onlinelibrary.wiley.com/doi/10.1002/dvdy.70200 by Naturalis Biodiversity Center, Wiley Online Library on [10/11/2026]. See the Terms and Conditions (https://onlinelibrary.wiley.com/terms-and-conditions) on Wiley Online Library for rules of use; OA articles are governed by the applicable Creative Commons License

Active ameloblasts overcome P deficiency

Vectorial ion transport is a basic function of epithelial cells. Accordingly, *slc34a2b* expression has been found in the skin and gill epithelium of the goldfish (*Carassius auratus*) and in the gill epithelium of its smaller relative, the zebrafish.[23] Ameloblasts are epithelial cells that transport minerals for enamel or enameloid mineralization. Subsequently, the cells actively remove proteins from the enamel/enameloid matrix.[22,32,33] Both functions have also been assigned to ameloblasts in teleosts.[34,35] This study demonstrates that the inner dental epithelium (ameloblasts) of the zebrafish also expresses the vectorial Na-P co-transporter *slc34a2b*. Similar to other Slc34 family transporters, Slc34a2b can secrete and reabsorb P.[36] The function of these transporters has been characterized in ameloblasts of mice.[22,32] Thus, we hypothesize that active P transport by ameloblasts can possibly explain the observed unaffected mineralization of enameloid in zebrafish under conditions of low dietary P intake. In Atlantic salmon, fed a low P diet with the same P level as in the current study, inorganic plasma phosphate (Pi) drops from over 4 mmol/L to under 2 mmol/L.[5] While we were unable to measure plasma Pi levels in LP zebrafish, it can be assumed that Pi levels are similarly low. The reduced plasma Pi level in salmon is still within the range of active P transport by the Na-P co-transporter Slc34a2 determined for Pacific hagfish (*Eptatretus stoutii*).[21] That *Slc34a2* expression is also found in the skin of hagfish is possibly an ancient character, given that the function of the integument is highly conserved across vertebrates.[37] Schultz et al. reason that, for a dermal skeleton that could have served as phosphorus storage, constant epithelial P-transport would have been required.[21] John Maisey argues along the same lines emphasizing that ameloblastic hypermineralization could have provided a mechanism for rapid hydroxyapatite assimilation and that the most primitive vertebrate hard tissue could have been a hypermineralized enamel-like substance, the product of ectodermal ameloblasts.[6] In mammals, that retain teeth as elements of the dermal skeleton, ectodermal *Slc34a2* expression is restricted to ameloblasts.[22,32]

Ameloblast-assisted dentin mineralization?

The unaffected mineralization of enameloid under conditions of low dietary P intake can potentially be explained with P transport by ameloblasts, as hypothesized above. More difficult to understand is the ongoing dentin mineralization under P-deficient conditions, while bone mineralization is arrested. In line with our findings on bone,[3,4] the study by Murshed et al. on mice has shown that low plasma P levels completely inhibit bone mineralization.[38] Yet, dentin and bone are closely related, with a range of intermediate tissues existing between bone and dentin, especially across non-tetrapods. Examples are osteodentin, mesodentin (dentin with enclosed odontocytes), atubular dentin, acellular bone, acellular cementum, or bone with dentin-like canaliculi of Williamson.[7,18] Accordingly, mechanisms of dentin and bone mineralization, albeit still being discussed, are assumed to be similar.[39] Different from ameloblasts and other epithelial cells, osteoblasts and odontoblasts, and thus also the cells with intermediate odontoblast/osteoblast characters that produce the pedicel,[18,40] have no vectorial P transporters from the SLC34A family. Housekeeping for cellular phosphate is achieved with the ubiquitously expressed SLC20A1 and SLC20A2 phosphate co-transporters.[41] At the same time the cells maintain an intracellular calcium concentration that is 10.000 times lower than extracellular calcium.[42] Because extracellular fluids are supersaturated for calcium and phosphate ions, osteoblasts and odontoblasts must produce mineralization inhibitors, such as matrix gla protein (MGP) and pyrophosphate, in order to prevent spontaneous mineralization.[39,42–45] Subsequently, the cells control mineralization by enzymatic removal of pyrophosphate from the matrices, presumably by tissue non-specific alkaline phosphatase (TNALP). Classic and recent studies on a cell-free bone model support previous findings about a collagen-induced precipitation of calcium and phosphate.[38,46,47] In the current experiment, dentin in LP zebrafish becomes increasingly mineralized during the life span of the tooth, albeit that mineralization is delayed. Continuous increase of dentin mineralization is also a character of mammalian teeth.[48] Given the admixture of matrices at the enameloid-dentin boundary,[49] and the reported presence of a thin layer of collar enameloid around the dentin,[19] we hypothesize that active mineral transport by ameloblasts possibly contributes to dentin mineralization. This could explain why, different from bone mineralization, LP conditions do not prevent dentin mineralization. Of significance, P deposition into dentin via enamel has been shown in experiments on mammalian teeth with radioactive P.[50]

Not addressed in this study are differences in dentin and bone mineralization that could relate to intrinsic characters of bone and dentin matrices. In mammals the concentration of dentin sialoprotein (DSP) is 400 times higher in dentin compared to bone matrix.[51] DSP derives from dentin sialophosphoprotein (DSPP), a secretory calcium binding protein (SCPP) group member. DSPP is an odontoblast intracellular protein that is cleaved into secreted proteins, dentin sialoprotein (DSP) and dentin phosphoprotein (DPP). DSP contains binding and affinity

10970177, 0, Downloaded from https://anatomypubs.onlinelibrary.wiley.com/doi/10.1002/dvdy.70200 by Naturalis Biodiversity Center, Wiley Online Library on [10/11/2026]. See the Terms and Conditions (https://onlinelibrary.wiley.com/terms-and-conditions) on Wiley Online Library for rules of use; OA articles are governed by the applicable Creative Commons License

domains for hydroxyapatite crystals and collagen fibers, respectively. It is the most phosphorylated protein in vertebrates.[52] DSPP mutations, and thus a lack of DSP, cause dentinogenesis imperfecta type 2, characterized by dentin hypomineralization.[53] Yet, no *dspp* orthologues have been found in zebrafish and other teleost fish.[54] Morita and colleagues observed that in zebrafish the expression patterns of secretory calcium-binding phosphoprotein 1 and 5 (*scpp1*, *scpp5*) are similar to those of *Dspp* gene expression in rats and mice, suggesting a related function.[55] Still, and despite similar genomic positions of zebrafish *scpp1* and rodent *Dspp*, the amino acid sequences differ considerably. Kawasaki et al. suggest a co-evolution of *scpp* genes and enamel, respectively enameloid.[19] Promotion of dentin mineralization by *Scpp* derivatives in zebrafish is a reasonable assumption but the underlying mechanisms require more investigations, particularly if zebrafish would be considered as a model for DSP-related mammalian dentinogenesis imperfecta.

Reduced mineralization under natural conditions

In the current experiment, teeth from animals that received a low-P diet displayed delayed dentin mineralization while the pedicel ("bone of attachment") and the subjacent bone remained non-mineralized. Uncoupled tooth and jaw bone mineralization resembles an early gnathostome condition with fully mineralized teeth that could be associated with non-mineralized cartilaginous jaw elements.[56] There are also numerous examples of extant teleosts with non-mineralized tooth attachment. Teeth can be firmly ankylosed but in several species flexible, non-mineralized tooth attachment facilitates tooth rotation.[57,58] In Atlantic salmon that suffer from starvation-related P-deficiency during their laborious upstream spawning migration, tooth development and replacement continue uninterrupted.[59] New teeth are fully mineralized but the tooth bases remain non-mineralized and teeth are replaced before a mineralized ankylosis is formed.[60] Deep-sea fish from the family Stomiidae combine a low mineralized endoskeleton with functional, enameloid-covered, fang-shaped teeth.[61] Animals from this family also have teeth with non-mineralized bases and teeth can be ankylosed to non-mineralized pharyngeal arch elements.[62,63]

CONCLUSION

Previous and current experiments on zebrafish, but also previous experiments with Atlantic salmon show pronounced mineralization defects related to low dietary P intake. Bone mineralization is impaired but bone matrix formation continues. Arguably, matrix deposition, and the formation of a bony skeletal element can be uncoupled from its mineralization. This study shows that in zebrafish tooth organogenesis and tooth replacement continue under conditions of low dietary P intake. In contrast to bone, teeth do mineralize. Mineralization of dentin is delayed but not arrested while enameloid mineralization is unaffected by low dietary P intake. It is hypothesized that, like in mammals, active ion transport by epithelial cells, that is, the ameloblasts, facilitates enameloid mineralization and possibly contributes to the mineralization of dentin.

EXPERIMENTAL PROCEDURES

Zebrafish maintenance and ethical statement

Wild type (WT) AB zebrafish (*Danio rerio*) were obtained from the European Zebrafish Research Center (Eggenstein-Leopoldshafen, Germany). The reporter zebrafish line *osc*:GFP was obtained from Dr. A. Willaert, Ghent University Hospital, Ghent.[4,64] WT and transgenic zebrafish embryos were raised under standard conditions.[4] Prior to the start of the feeding trial, animals were fed for 1 week three times a day with a regular phosphorus (RP) diet.[3] The nutrition trial started at 28 days post-fertilization (dpf): fish were randomly divided in three groups, grown in tanks with a density of 10 fish/L and fed three times a day with a low phosphorus (LP), a regular phosphorus (RP) and a high phosphorus (HP) diet, respectively (see below for details).[3] Samples were collected before the start of the experiment (T0 samples, 28 dpf), after 1 month and after 2 months of dietary treatment (2 and 3 months post-fertilization, respectively). Animal care, experimentation and euthanasia complied with EU Directive 2010/63/EU. The experimental protocol was approved by the Italian Ministry of Health (approval animal protocol no. 260/2020-PR, 26 March 2020).

Diet composition

Diet composition (Table S3) and nutritional experiment are described in detail in Cotti et al.[3] Briefly, the diets were formulated to have a total P content of 0.5%, 1.0% and 1.5%, termed low P (LP) diet, regular P (RP) diet and high P (HP) diet, respectively. Monoammonium phosphate ($NH_4H_2PO_4$, MAP) was used as dietary inorganic P

10970177, 0, Downloaded from https://anatomypubs.onlinelibrary.wiley.com/doi/10.1002/dvdy.70200 by Naturalis Biodiversity Center, Wiley Online Library on [10/11/2026]. See the Terms and Conditions (https://onlinelibrary.wiley.com/terms-and-conditions) on Wiley Online Library for rules of use; OA articles are governed by the applicable Creative Commons License

supplement.[2,65] To keep all diets equal in nutrients, except for P concentration, MAP replaced the inert filler diatomaceous earth (Diamol, Imerys, Denmark). The diets were formulated by SimplyFish AS (Stavanger, Norway, www.simplyfish.no) and by the Danish Technological Institute (Taastrup, Denmark, https://www.dti.dk). The P content of the product was verified at the University of Hohenheim (Stuttgart, Germany, https://www.uni-hohenheim.de) and determined with 5.04, 9.84 and 14.64 g/kg diet for the LP, RP, and HP diet, respectively.

Whole mount staining with Alizarin red S

WT zebrafish of 28 dpf ($n = 8$), one month treated (LP $n = 18$, RP $n = 16$, HP $n = 18$) and 2 months treated (LP $n = 20$, RP $n = 20$, HP $n = 20$) animals were euthanized by an overdose (0.3%) of tricaine (3-amino benzoic acid ethyl ester), and fixed for 24 h in 4% paraformaldehyde (PFA) in 1× phosphate-buffered saline (PBS) at 4°C. Whole mount-staining with Alizarin red S was done according to the protocol by Taylor and Van Dyke.[66] The pharyngeal dentition was dissected, analyzed, and imaged using an Axio Zoom V16 stereomicroscope (Carl Zeiss, Oberkochen, Germany) with oblique illumination and equipped with a 5MP CCD camera. Based on Alizarin red S staining, dentin and pedicel of the ventral teeth (10 teeth per specimen analyzed in total) were qualitatively evaluated as mineralized (positively stained) or non-mineralized (unstained). The total number of teeth analyzed for mineralization after 30 and 60 days of dietary treatment (ddt) was 1120: LP group: 30 ddt, 180 teeth examined; 60 ddt, 200 teeth examined. RP group: 30 ddt, 160 teeth examined; 60 ddt, 200 teeth examined. HP group: 30 ddt, 180 teeth examined; 60 ddt, 200 teeth examined. Replacement teeth not attached to the pharyngeal bone were considered young, yet non-functional teeth. Enameloid remains unstained because the hypermineralized matrix is not accessible for Alizarin red S and other dyes.[67,68] Ventral images of the ventral teeth 1V, 2V, and 3V were used to measure dentin thickness at half of the total tooth height, from the tip to the base, using ImageJ software (NIH, Bethesda, MD, USA). Dentin thickness was normalized to the total tooth height. The strongly curved teeth 4V and 5V were not considered in this analysis.[14]

Histological analysis

WT specimens for histological analysis (LP $n = 2$, RP $n = 2$, HP $n = 2$) were euthanized by tricaine overdose, and fixed for 24 h in 2.5% PFA, 1.5% glutaraldehyde, 0.1 M sodium cacodylate buffer (pH 7.4) and 0.001% $CaCl_2$ at 4°C. Bone mineral detection was carried out on histological sections obtained from non-decalcified specimens embedded in glycol methacrylate.[69] Cross sections of 3 µm were cut on a Microm HM 360 (Marshall Scientific, Hampton, NH, USA) automated microtome and were stained following the Von Kossa/Van Gieson staining protocol.[70] Images were acquired using an Axio Imager-Z1 microscope (Carl Zeiss, Oberkochen, Germany) equipped with an Axiocam 503 color camera (Carl Zeiss, Oberkochen, Germany).

After 2 months of dietary treatment, *osc*:GFP zebrafish (LP $n = 3$, RP $n = 3$, HP $n = 3$) were euthanized by tricaine overdose. To preserve and visualize GFP on sections, we followed the protocol from Oralová et al.[71] Briefly, *osc*:GFP zebrafish were fixed for 2 h in 4% PFA in 1× PBS, pH 7.4, at room temperature (RT), rinsed in tap water for 1 h and decalcified for 48 h in 10% EDTA, 4% PFA, pH 7.4. After rinsing 1 h in tap water, samples were embedded in glycol methacrylate.[69] Cross sections of 3 µm were cut on a Microm HM 360 (Marshall Scientific, Hampton, NH, USA) automated microtome. Images were acquired using an Axio Imager-Z1 microscope (Carl Zeiss, Oberkochen, Germany). To measure the fluorescent signal within the tooth pulp cavity, a replacement tooth and a young functional tooth in the same position in all three dietary groups were selected based on characteristics of the pulp.[72] Images of the complete series of sections of the selected teeth were used to quantify the fluorescence signal within the pulp cavity using the ZF BONE ImageJ toolkit.[73] The signal area was normalized to the pulp cavity area in all the sections.

Micro CT and synchrotron X-ray tomographic microscopy

Overview scans to show the localization and shape of the pharyngeal jaws and the orientation of the teeth were obtained with the Zeiss Xradia S20 Versa Micro CT scanner (Carl Zeiss, Oberkochen, Germany) at a voxel size of 4 µm.[74]

WT fish fed the experimental diets for 2 months ($n = 1$ fish per dietary group) were euthanized by tricaine overdose, fixed for 24 h in 2.5% PFA, 1.5% glutaraldehyde, 0.1 M sodium cacodylate buffer (pH 7.4) and 0.001% $CaCl_2$ at 4°C and were dehydrated in a graded series of ethanol. Alizarin red S analysis of the abdominal and the caudal part of the body confirmed that animals selected for synchrotron X-ray tomographic microscopy had responded to the diets. Synchrotron X-ray tomographic microscopy of the pharyngeal jaws was performed at the TOMCAT beamline (X02DA) (Swiss Light

10970177, 0, Downloaded from https://anatomypubs.onlinelibrary.wiley.com/doi/10.1002/dvdy.70200 by Naturalis Biodiversity Center, Wiley Online Library on [10/11/2026]. See the Terms and Conditions (https://onlinelibrary.wiley.com/terms-and-conditions) on Wiley Online Library for rules of use; OA articles are governed by the applicable Creative Commons License

Source (SLS), Paul Scherrer Institut (PSI), Villigen, Switzerland). Scans were acquired with 1501 projections over 180° at 16 keV with an exposure time of 150 ms using a 10× objective resulting in an effective voxel size of 0.65 μm.[3] Radiographs were phase-retrieved using the Paganin algorithm, tomographically reconstructed and subsequently analyzed using Amira 3.1.1 software (Thermo Fisher, Waltham, MA, USA). The hypermineralized enameloid, the mineralized dentin and pedicel of the ventral tooth 1V, as well as the mineralized parts of the supporting pharyngeal bone, were identified applying constant greyscale-thresholds to all samples. Any non-mineralized matrix was manually identified and selected on each projection. The resulting segmentations and virtual sections of the ventral tooth 1V in LP, RP and HP fish were used to visualize the mineralized and non-mineralized dentin, pedicel and pharyngeal bone.

The samples processed for synchrotron X-ray tomography were subsequently embedded in epon,[75] serially sectioned at 1 μm thickness on a Microm HM 360 automated microtome using a diamond knife and stained with toluidine blue.

In situ hybridization

WT 2 months treated zebrafish ($n = 2$ per dietary group) were fixed for 2 h at RT in 4% PFA in 1× PBS in DEPC-dH_2O, washed with 1× PBS in DEPC-dH_2O, dehydrated through a 1× PBS in DEPC-dH_2O/methanol gradient and stored in 100% methanol at −20°C. Prior to in situ hybridization, pharyngeal jaws were dissected from each specimen. For in situ hybridization, a 311 bp amplicon from the zebrafish *slc34a2b* mRNA (NM_182877.2) was amplified from zebrafish cDNA (primer sequences: forward 5′-GAATCGCAAACTGCACTCCG-3′; reverse 5′-GAGGATGGCCAGGTATCCTG-3′) using Taq polymerase Kit (Invitrogen, Waltham, MA, USA). The obtained PCR product was cloned into pCR4-TOPO vector using the TOPO TA Cloning Kit for Sequencing (Invitrogen, Waltham, MA, USA). The sequence of the cloned PCR product was confirmed by sequencing. Sense and antisense RNA probes were generated from 1 μg of linearized vector using MAXIscript™ T7/T3 Kit (Invitrogen, Waltham, MA, USA) and labeled with digoxigenin-dUTP of the DIG RNA labeling kit (Roche Diagnostics, Mannheim, Germany). RNA probes were treated with RNase-free DNase, recovered by ethanol precipitation according to manufacturer's instructions and stored at −80°C. Whole mount in situ hybridization was performed following the protocol described in Verstraeten et al.[75] Following whole mount in situ hybridization, the dissected pharyngeal jaws were embedded in glycol methacrylate. Cross sections of 3 μm were cut, mounted and analyzed using an Axio Imager-Z1 microscope.

Raman micro-spectroscopy

The macromolecular composition of the mineral- and collagen phase was evaluated by Raman micro-spectroscopy (inVia, Renishaw). Three zebrafish per group were fixed in 4% PFA in 1x PBS for 24 h, subsequently underwent stepwise dehydration in increasing concentrations of ethanol, and were embedded in polymethyl methacrylate (PMMA). Sample blocks were polished coplanar for tissue composition analysis, whereby the transversal plane of the skull was exposed and the cross-sectional plane of the tooth 2V was selected as the region of interest. Within each of the different dental tissues, a rectangular 2D map was acquired with a step size of 1.5 μm and dimensions of 18 × 20 μm for enameloid, 50 × 30 μm for dentin, 20 × 28 μm for pedicel, and 25 × 20 μm for pharyngeal bone. Raman spectra were acquired with a 785 nm laser, within a spectral range of 300–1800 cm^{-1}, grating of 1200 l/mm, 50× objective and a laser spot size of 1 μm, a laser intensity of 22.4 mW measured without objective, and an exposure time of 10 ms with two accumulations per laser spot. Spectral processing included polynomial baseline correction, subtraction from the PMMA signal and averaging of spectra per region (WiRE, Renishaw). According to established protocols, several Raman parameters were determined.[31,76] Mineral-to-matrix ratios were determined based on dividing peak areas (phosphate ν_1PO_4 at 961 cm^{-1}, carbonate at 1071 cm^{-1}, amide III at 1243 cm^{-1}, CH_2 at ∼1450 cm^{-1}) and mineral crystallinity was assessed as the inverse of the full-width-half-maximum of the phosphate peak.

Nanoindentation

Mechanical properties were assessed in three tissues, that is, dentin, pedicel and pharyngeal bone of the tooth 2V from three fish per dietary group (Figure 3G for locations). Briefly, fish were embedded in PMMA, ground coplanar until the tooth of interest was exposed, and polished with 3 and 1 μm diamond suspension followed by final polishing with 0.05 μm aluminium-oxide suspension. Indentations were performed in depth-sensing continuous stiffness mode with a final depth of 300 nm. The nanoindenter (Nano Indenter G200 equipped with a Berkovich diamond tip, Keysight Technologies, Santa Rosa, CA, USA) was calibrated on fused silica before and after each measurement. Based on the Oliver and Pharr

10970177, 0, Downloaded from https://anatomypubs.onlinelibrary.wiley.com/doi/10.1002/dvdy.70200 by Naturalis Biodiversity Center, Wiley Online Library on [10/11/2026]. See the Terms and Conditions (https://onlinelibrary.wiley.com/terms-and-conditions) on Wiley Online Library for rules of use; OA articles are governed by the applicable Creative Commons License

method[77] and by applying a Poisson's ratio of 0.3, the mechanical properties elastic modulus (E) and hardness (H) in the different regions were determined using in-house software (NanoSuite, Keysight Technologies, Santa Rosa, CA, USA).

Statistical analysis

Quantitative variables are expressed as mean ± standard deviation, categories are expressed as percentages. Statistical analysis was performed using Past4.04 software.[78] Differences in the extent of mineralization of young non-functional teeth and in the pedicel were evaluated by means of a Chi-square test followed by Bonferroni correction. Comparison of dentin thickness in ventral teeth was based on the non-parametric Mann–Whitney test followed by Bonferroni correction. Differences in the *osc*: GFP fluorescence signal were based on the Student's *t*-test followed by Bonferroni correction. Effects of different dietary P-content and in the composition of the mineral- and collagen phase and in the mechanical properties of the dental tissues were based on Two-Way ANOVA followed by Tukey's multiple comparisons tests. A *p*-value less than .05 was considered significant.

ACKNOWLEDGMENTS

SC, PEW and AH acknowledge funding by the European Union's Horizon 2020 Research and Innovation Programme under the Marie Skłodowska-Curie grant agreement no. 766347 (Biomedaqu) and by Ghent University, Bijzonder Onderzoeksfonds grant code BOF. ITN.2021.0012.01. SC acknowledges travel grants from Facultaire Commissie Wetenschappelijk Onderzoek (FCWO) of Ghent University and from Research Foundation Flanders (FWO, grant number K200621N). We acknowledge the animal facility "Centro di servizio per la gestioneunificata delle attività di stabulazione e di radiobiologia" of the University of Pavia, Pavia, Italy, where animals of some experiments were hosted; the OPBA of the University of Pavia for support in animal protocol drawing up. We acknowledge the Paul Scherrer Institut, Villigen, Switzerland for provision of synchrotron radiation beamtime at the TOMCAT beamline of the SLS and the micro CT facility at Naturalis Biodiversity Center, Leiden, The Netherlands for scan time using the Zeiss Xradia 520 Versa. SC, PEW, and AF are members of the International Scientific Society of Ectopic Calcification (ISSEC). PEW and AF are members of the International Network on Ectopic Calcification (INTEC).

CONFLICT OF INTEREST STATEMENT

The authors declare no conflicts of interest.

DATA AVAILABILITY STATEMENT

The data that support the findings of this study are available from the corresponding author, upon reasonable request.

ORCID

S. Cotti https://orcid.org/0000-0001-5143-5563
A. Huysseune https://orcid.org/0000-0001-8713-0462
I. A. K. Fiedler https://orcid.org/0000-0003-2724-258X
B. Busse https://orcid.org/0000-0002-3099-8073
C. Di Biagio https://orcid.org/0000-0001-9096-3166
M. Rücklin https://orcid.org/0000-0002-7254-837X
F. Marone https://orcid.org/0000-0002-3467-8763
A. Forlino https://orcid.org/0000-0002-6385-1182
P. E. Witten https://orcid.org/0000-0002-2928-5762

REFERENCES

1. Witten PE, Owen MA, Fontanillas R, Soenens M, McGurk C, Obach A. A primary phosphorus-deficient skeletal phenotype in juvenile Atlantic salmon *Salmo salar*: the uncoupling of bone formation and mineralization. *J Fish Biol*. 2016;88(2):690-708. doi:10.1111/jfb.12870132
2. Witten PE, Fjelldal PG, Huysseune A, McGurk C, Obach A, Owen MAG. Bone without minerals and its secondary mineralization in Atlantic salmon. *J Exp Biol*. 2019;222(3):jeb188763. doi:10.1242/jeb.188763
3. Cotti S, Huysseune A, Koppe W, et al. More bone with less minerals? The effects of dietary phosphorus on the post-cranial skeleton in zebrafish. *Int J Mol Sci*. 2020;21(15):5429. doi:10.3390/ijms21155429
4. Cotti S, Di Biagio C, Huysseune A, Koppe W, Forlino A, Witten PE. Matrix first, minerals later: fine-tuned dietary phosphate increases bone formation in zebrafish. *JBMR Plus*. 2024;8(8):ziae081. doi:10.1093/jbmrpl/ziae081
5. Drábiková L, Fjelldal PG, Yousaf MN, et al. Elevated water CO_2 can prevent dietary-induced osteomalacia in post-smolt Atlantic Salmon (*Salmo salar*, L.). *Biomolecules*. 2023;13(4):663. doi:10.3390/biom13040663
6. Maisey JG. Phylogeny of early vertebrate skeletal induction and ossification patterns. In: Hecht MK, Wallace B, Prance GT, eds. *Evolutionary Biology*. Springer US; 1988:1-36. doi:10.1007/978-1-4613-0931-4_1
7. Hall BK, Witten PE. Plasticity of and transitions between skeletal tissues in vertebrate evolution and development. In: Anderson JS, Sues HD, eds. *Major Transitions in Vertebrate Evolution*. Indiana University Press; 2007:13-59.
8. Haridy Y, Osenberg M, Hilger A, Manke I, Davesne D, Witzmann F. Bone metabolism and evolutionary origin of osteocytes: novel application of FIB-SEM tomography. *Sci Adv*. 2021;7(14):eabb9113. doi:10.1126/sciadv.abb9113
9. Karshan M. Calcification of teeth and bones on rachitic and non-rachitic diets. *J Dent Res*. 1933;13(4):301-304. doi:10.1177/00220345330130040801
10. Karshan M, Rosebury T. Correlation of chemical and pathological changes in teeth and bones on rachitic and non-rachitic diets. *J Dent Res*. 1933;13(4):305-310. doi:10.1177/00220345330130040901

10970177, 0, Downloaded from https://anatomypubs.onlinelibrary.wiley.com/doi/10.1002/dvdy.70200 by Naturalis Biodiversity Center, Wiley Online Library on [10/11/2026]. See the Terms and Conditions (https://onlinelibrary.wiley.com/terms-and-conditions) on Wiley Online Library for rules of use; OA articles are governed by the applicable Creative Commons License

11. Gaunt WE, Irving JT. The influence of dietary calcium and phosphorus upon tooth formation. *J Physiol*. 1940;99(1):18-29. doi:10.1113/jphysiol.1940.sp003875
12. Witten PE, Harris MP, Huysseune A, Winkler C. Small teleost fish provide new insights into human skeletal diseases. *Methods Cell Biol*. 2017;138:321-346. doi:10.1016/bs.mcb.2016.09.001
13. Huysseune A, Delgado S, Witten PE. How to replace a tooth: fish(ing) for answers. *Oral Biosci Med*. 2005;2(2/3):75-81.
14. Wautier K, Van der heyden C, Huysseune A. A quantitative analysis of pharyngeal tooth shape in the zebrafish (*Danio rerio*, Teleostei, Cyprinidae). *Arch Oral Biol*. 2001;46(1):67-75. doi:10.1016/s0003-9969(00)00091-1
15. Huysseune A, Van der heyden C, Sire J-Y. Early development of the zebrafish (*Danio rerio*) pharyngeal dentition (Teleostei, Cyprinidae). *Anat Embryol (Berl)*. 1998;198(4):289-305. doi:10.1007/s004290050185
16. Van der heyden C, Huysseune A, Sire JY. Development and fine structure of pharyngeal replacement teeth in juvenile zebrafish (*Danio rerio*) (Teleostei, Cyprinidae). *Cell Tissue Res*. 2000;302(2):205-219. doi:10.1007/s004410000180
17. Van der heyden C, Huysseune A. Dynamics of tooth formation and replacement in the zebrafish (*Danio rerio*) (Teleostei, Cyprinidae). *Dev Dyn*. 2000;219(4):486-496. doi:10.1002/1097-0177(2000)9999:99993.0.CO;2-Z
18. Rosa JT, Witten PE, Huysseune A. Cells at the edge: the dentin–bone interface in zebrafish teeth. *Front Physiol*. 2021;12:723210. doi:10.3389/fphys.2021.723210
19. Kawasaki K, Keating JN, Nakatomi M, et al. Coevolution of enamel, ganoin, enameloid, and their matrix SCPP genes in osteichthyans. *iScience*. 2021;24(1):102023. doi:10.1016/j.isci.2020.102023
20. Papagerakis P, Berdal A, Mesbah M, et al. Investigation of osteocalcin, osteonectin, and dentin sialophosphoprotein in developing human teeth. *Bone*. 2002;30(2):377-385. doi:10.1016/S8756-3282(01)00683-4
21. Schultz AG, Guffey SC, Clifford AM, Goss GG. Phosphate absorption across multiple epithelia in the Pacific hagfish (*Eptatretus stoutii*). *Am J Physiol Integr Comp Physiol*. 2014;307(6):R643-R652. doi:10.1152/ajpregu.00443.2013
22. Merametdjian L, Beck-Cormier S, Bon N, et al. Expression of phosphate transporters during dental mineralization. *J Dent Res*. 2017;97(2):209-217. doi:10.1177/0022034517729811
23. Verri T, Werner A. Type II Na+ −phosphate cotransporters and phosphate balance in teleost fish. *Pflugers Arch*. 2019;471(1):193-212. doi:10.1007/s00424-018-2239-4
24. Witten PE, Huysseune A. A comparative view on mechanisms and functions of skeletal remodelling in teleost fish, with special emphasis on osteoclasts and their function. *Biol Rev Camb Philos Soc*. 2009;84(2):315-346. doi:10.1111/j.1469-185X.2009.00077.x
25. Dean MN, Ekstrom L, Monsonego-Ornan E, et al. Mineral homeostasis and regulation of mineralization processes in the skeletons of sharks, rays and relatives (Elasmobranchii). *Semin Cell Dev Biol*. 2015;46:51-67. doi:10.1016/j.semcdb.2015.10.022
26. Lall SP. Chapter 6 – The minerals. In: Hardy RW, Kaushik SJ, eds. *Fish Nutrition*. fourth ed. Academic Press; 2022:469-554. doi:10.1016/B978-0-12-819587-1.00005-7
27. Bonjour JP. Calcium and phosphate: a duet of ions playing for bone health. *J Am Coll Nutr*. 2011;30(5 Suppl 1):438S-448S. doi:10.1080/07315724.2011.10719988
28. Huitema LF, Apschner A, Logister I, et al. Entpd5 is essential for skeletal mineralization and regulates phosphate homeostasis in zebrafish. *Proc Natl Acad Sci U S A*. 2012;109(52):21372-21377. doi:10.1073/pnas.1214231110
29. Foster BL, Nociti FH Jr, Somerman MJ. The rachitic tooth. *Endocr Rev*. 2014;35(1):1-34. doi:10.1210/er.2013-1009
30. Donnelly E, Chen DX, Boskey AL, Baker SP, van der Meulen MCH. Contribution of mineral to bone structural behavior and tissue mechanical properties. *Calcif Tissue Int*. 2010;87(5):450-460. doi:10.1007/s00223-010-9404-x
31. Fiedler IAK, Schmidt FN, Wölfel EM, et al. Severely impaired bone material quality in *Chihuahua* zebrafish resembles classical dominant human osteogenesis imperfecta. *J Bone Min Res*. 2018;33(8):1489-1499. doi:10.1002/jbmr.3445
32. Onishi T, Okawa R, Ogawa T, Shintani S, Ooshima T. *Phex* mutation causes the reduction of *Npt2b* mRNA in teeth. *J Dent Res*. 2007;86(2):158-162. doi:10.1177/154405910708600210
33. Bartlett JD. Dental enamel development: proteinases and their enamel matrix substrates. *ISRN – Dent*. 2013;2013:684607. doi:10.1155/2013/684607
34. Sasagawa I. Mechanism of mineralization in the enameloid of elasmobranchs and teleosts. *Connect Tissue Res*. 1988;39(1–3):207-214. doi:10.3109/03008209809023928
35. Sasagawa I, Ishiyama M, Akai J. Cellular influence in the formation of enameloid during odontogenesis in bony fishes. *Mater Sci Eng C*. 2006;26(4):630-634. doi:10.1016/j.msec.2005.04.010
36. Gupta A, Renfro JL. Control of phosphate transport in flounder renal proximal tubule primary cultures. *Am J Physiol*. 1989;256(4):R850-R857. doi:10.1152/ajpregu.1989.256.4.R850
37. Miller CT, Archambeault SL, Square TA. Fishing for the secrets of vertebrate integument development, regeneration, and evolution. *Am J Biol Anthropol*. 2022;177(suppl 73):125. doi:10.1002/ajpa.24515
38. Murshed M, Harmey D, Millán JL, McKee MD, Karsenty G. Unique coexpression in osteoblasts of broadly expressed genes accounts for the spatial restriction of ECM mineralization to bone. *Genes Dev*. 2005;19(9):1093-1104. doi:10.1101/gad.1276205
39. Omelon S, Ariganello M, Bonucci E, Grynpas M, Nanci A. A review of phosphate mineral nucleation in biology and geobiology. *Calcif Tissue Int*. 2013;93(4):382-396. doi:10.1007/s00223-013-9784-9
40. Šulcová M, Dumková J, Hutečková B, et al. Tooth–bone attachment tissue is produced by cells with a mixture of odontoblastic and osteoblastic features in reptiles. *J Anat*. 2026;248(2):251-268. doi:10.1111/joa.70059
41. Hernando N, Gagnon K, Lederer E. Phosphate transport in epithelial and nonepithelial tissue. *Physiol Rev*. 2020;101(1):1-35. doi:10.1152/physrev.00008.2019
42. Golub EE. Biomineralization and matrix vesicles in biology and pathology. *Semin Immunopathol*. 2011;33(5):409-417. doi:10.1007/s00281-010-0230-z
43. Boskey AL. The role of extracellular matrix components in dentin mineralization. *Crit Rev Oral Biol Med*. 1991;2(2):369-387. doi:10.1177/10454411910020030501
44. Ortiz-Delgado JB, Simes DC, Gavaia P, Sarasquete C, Cancela ML. Osteocalcin and matrix GLA protein in developing teleost teeth: identification of sites of mRNA and protein

10970177, 0, Downloaded from https://anatomypubs.onlinelibrary.wiley.com/doi/10.1002/dvdy.70200 by Naturalis Biodiversity Center, Wiley Online Library on [10/11/2026]. See the Terms and Conditions (https://onlinelibrary.wiley.com/terms-and-conditions) on Wiley Online Library for rules of use; OA articles are governed by the applicable Creative Commons License

accumulation at single cell resolution. *Histochem Cell Biol*. 2005;124(2):123-130. doi:10.1007/s00418-005-0015-y

45. Narisawa S, Harmey D, Yadav MC, O'Neill WC, Hoylaerts MF, Millán JL. Novel inhibitors of alkaline phosphatase suppress vascular smooth muscle cell calcification. *J Bone Miner Res*. 2007;22(11):1700-1710. doi:10.1359/jbmr.070714
46. Glimcher MJ, Hodge AJ, Schmitt FO. Macromolecular aggregation states in relation to mineralization: the collagen-hydroxyapatite system as studied in vitro. *Proc Natl Acad Sci U S A*. 1957;43(10):860-867. doi:10.1073/pnas.43.10.860
47. van der Meijden RHM, Daviran D, Rutten L, et al. A 3D cell-free bone model shows collagen mineralization is driven and controlled by the matrix. *Adv Funct Mater*. 2023;33(42):2212339. doi:10.1002/adfm.202212339
48. Balic A. Biology explaining tooth repair and regeneration: a mini-review. *Gerontology*. 2018;64(4):382-388. doi:10.1159/000486592
49. Huysseune A, Sire JY. Evolution of patterns and processes in teeth and tooth-related tissues in non-mammalian vertebrates. *Eur J Oral Sci*. 1998;106(Suppl):437-481. doi:10.1111/j.1600-0722.1998.tb02211.x
50. Barnum CP, Armstrong WD. In vivo and in vitro exchange of phosphorus by enamel and dentin. *Am J Physiol*. 1941;135(2):478-484. doi:10.1152/ajplegacy.1941.135.2.478
51. Kawasaki K, Weiss KM. SCPP gene evolution and the dental mineralization continuum. *J Dent Res*. 2008;87(6):520-531. doi:10.1177/154405910808700608
52. Riou MC, Touraivane S, Berdal A, et al. Physiology of dentinogenesis and pathophysiology of dentinogenesis imperfecta: how does it affect dentin structure and biomechanics? *Acta Biomater*. 2025;207:131-141. doi:10.1016/j.actbio.2025.10.009
53. Maciejewska I, Chomik E. Hereditary dentine diseases resulting from mutations in DSPP gene. *J Dent*. 2012;40(7):542-548. doi:10.1016/j.jdent.2012.04.004
54. Kawasaki K. The SCPP gene repertoire in bony vertebrates and graded differences in mineralized tissues. *Dev Genes Evol*. 2009;219(3):147-157. doi:10.1007/s00427-009-0276-x
55. Morita T, Matsumoto S, Baba O. Expression of secretory calcium-binding phosphoprotein (scpp) genes in medaka during the formation and replacement of pharyngeal teeth. *BMC Oral Health*. 2023;23(1):744. doi:10.1186/s12903-023-03498-7
56. Maisey JG, Turner S, Naylor GJP, Miller RF. Dental patterning in the earliest sharks: implications for tooth evolution. *J Morphol*. 2014;275(5):586-596. doi:10.1002/jmor.20242
57. Fink WL. Ontogeny and phylogeny of tooth attachment modes in actinopterygian fishes. *J Morphol*. 1981;167(2):167-184. doi:10.1002/jmor.1051670203
58. Berkovitz BKB, Shellis RP. *The Teeth of Non-Mammalian Vertebrates*. Elsevier Academic Press; 2016. doi:10.1016/C2014-0-02210-1
59. Witten PE, Hall BK. Seasonal changes in the lower jaw skeleton in male Atlantic salmon (*Salmo salar* L.): remodelling and regression of the kype after spawning. *J Anat*. 2003;203(5):435-450. doi:10.1046/j.1469-7580.2003.00239.x
60. Huysseune A, Hall BK, Witten PE. Establishment, maintenance and modifications of the lower jaw dentition of wild Atlantic salmon (*Salmo salar* L.) throughout its life cycle. *J Anat*. 2007;211(4):471-484. doi:10.1111/j.1469-7580.2007.00788.x
61. Schnell NK, Britz R, Johnson GD. New insights into the complex structure and ontogeny of the occipito-vertebral gap in barbeled dragonfishes (Stomiidae, Teleostei). *J Morphol*. 2010;271(8):1006-1022. doi:10.1002/jmor.10858
62. Schnell NK, Johnson GD. Ontogenetic fusion of the third and fourth pharyngobranchial in barbeled dragonfishes (Stomiidae, Teleostei) with a revision of the identity of the single posterior upper pharyngeal toothplate. *Copeia*. 2012;2012(3):394-407. doi:10.1643/CG-11-051
63. Schnell NK, Johnson GD. Evolution of a functional head joint in deep-sea fishes (Stomiidae). *PLoS One*. 2017;12(2):e0170224. doi:10.1371/journal.pone.0170224
64. Vanoevelen J, Janssens A, Huitema LFA, et al. Trpv5/6 is vital for epithelial calcium uptake and bone formation. *FASEB J*. 2011;25(9):3197-3207. doi:10.1096/fj.11-183145
65. Morales GA, Azcuy RL, Casaretto ME, et al. Effect of different inorganic phosphorus sources on growth performance, digestibility, retention efficiency and discharge of nutrients in rainbow trout (*Oncorhynchus mykiss*). *Aquaculture*. 2018;495:568-574. doi:10.1016/j.aquaculture.2018.06.036
66. Taylor WR, Van Dyke GC. Revised procedures for staining and clearing small fishes and other vertebrates for bone and cartilage study. *Cybium*. 1985;9(2):107-119.
67. Bruneel B, Mathä M, Paesen R, Ameloot M, Weninger WJ, Huysseune A. Imaging the zebrafish dentition: from traditional approaches to emerging technologies. *Zebrafish*. 2015;12(1):1-10. doi:10.1089/zeb.2014.0980
68. Mitsiadis TA, Jimenez-Rojo L, Balic A, Weber S, Saftig P, Pagella P. Adam10-dependent Notch signaling establishes dental epithelial cell boundaries required for enamel formation. *iScience*. 2022;25(10):105154. doi:10.1016/j.isci.2022.105154
69. Witten PE, Hansen A, Hall BK. Features of mono- and multinucleated bone resorbing cells of the zebrafish *Danio rerio* and their contribution to skeletal development, remodeling, and growth. *J Morphol*. 2001;250(3):197-207. doi:10.1002/jmor.1065
70. Humason GL, Presnell JK, Schreibman MP. *Humason's Animal Tissue Techniques*. Johns Hopkins University Press; 1997.
71. Oralová V, Rosa JT, Soenens M, et al. Beyond the whole-mount phenotype: high-resolution imaging in fluorescence-based applications on zebrafish. *Biol Open*. 2019;8(5):bio042374. doi:10.1242/bio.042374
72. Huysseune A. Formation of a successional dental lamina in the zebrafish (*Danio rerio*): support for a local control of replacement tooth initiation. *Int J Dev Biol*. 2006;50(7):637-643. doi:10.1387/ijdb.052098ah
73. Tarasco M, Cordelières FP, Cancela ML, Laizé V. ZFBONE: an ImageJ toolset for semi-automatic analysis of zebrafish bone structures. *Bone*. 2020;138:115480. doi:10.1016/j.bone.2020.115480
74. Kague E, Kwon RY, Busse B, Witten PE, Karasik D. Standardization of bone morphometry and mineral density assessments in zebrafish and other small laboratory fishes using X-ray radiography and micro-computed tomography. *J Bone Miner Res*. 2024;39(12):1695-1710. doi:10.1093/jbmr/zjae171

10970177, 0, Downloaded from https://anatomypubs.onlinelibrary.wiley.com/doi/10.1002/dvdy.70200 by Naturalis Biodiversity Center, Wiley Online Library on [10/11/2026]. See the Terms and Conditions (https://onlinelibrary.wiley.com/terms-and-conditions) on Wiley Online Library for rules of use; OA articles are governed by the applicable Creative Commons License

75. Verstraeten B, Sanders E, Huysseune A. Whole mount immunohistochemistry and in situ hybridization of larval and adult zebrafish dental tissues. In: Kioussi C, ed. *Odontogenesis: Methods and Protocols*. Humana Press; 2012:179-191. doi:10.1007/978-1-61779-860-3_16
76. Morris MD, Mandair GS. Raman assessment of bone quality. *Clin Orthop Relat Res*. 2011;469(8):2160-2169. doi:10.1007/s11999-010-1692-y
77. Oliver WC, Pharr GM. An improved technique for determining hardness and elastic modulus using load and displacement sensing indentation experiments. *J Mater Res*. 1992;7(6):1564-1583. doi:10.1557/JMR.1992.1564
78. Hammer Ø, Harper DAT, Ryan PD. Past: paleontological statistics software package for education and data analysis. *Palaeontol Electron*. 2001;4(1–4):1-9.

SUPPORTING INFORMATION

Additional supporting information can be found online in the Supporting Information section at the end of this article.

How to cite this article: Cotti S, Huysseune A, Fiedler IAK, et al. Different from bone: Tooth formation and enameloid mineralization are not affected by reduced dietary phosphorus intake. *Developmental Dynamics*. 2026;1-18. doi:10.1002/dvdy.70200

10970177, 0, Downloaded from https://anatomypubs.onlinelibrary.wiley.com/doi/10.1002/dvdy.70200 by Naturalis Biodiversity Center, Wiley Online Library on [10/11/2026]. See the Terms and Conditions (https://onlinelibrary.wiley.com/terms-and-conditions) on Wiley Online Library for rules of use; OA articles are governed by the applicable Creative Commons License